
AFRL-RX-WP-JA-2016-0328

# EFFECT OF IRREGULARITY IN SHAPE AND BOUNDARY OF A MACRO-TEXTURE REGION IN TITANIUM (POSTPRINT)

**James L. Blackshire and Shaun L. Freed**

**AFRL/RX**

**Jeong K. Na**

**Wyle**

**15 October 2015**
**Interim Report**



**(STINFO COPY)**

**AIR FORCE RESEARCH LABORATORY**
**MATERIALS AND MANUFACTURING DIRECTORATE**
**WRIGHT-PATTERSON AIR FORCE BASE, OH 45433-7750**
**AIR FORCE MATERIEL COMMAND**
**UNITED STATES AIR FORCE**

# REPORT DOCUMENTATION PAGE

*Form Approved*
*OMB No. 0704-0188*



| 1. REPORT DATE *(DD-MM-YY)* | 2. REPORT TYPE | 3. DATES COVERED *(From - To)* |
|---|---|---|
| 15 October 2015 | Interim | 2 October 2014 – 15 September 2015 |

**4. TITLE AND SUBTITLE**
EFFECT OF IRREGULARITY IN SHAPE AND BOUNDARY OF A MACRO-TEXTURE REGION IN TITANIUM (POSTPRINT)

**5a. CONTRACT NUMBER**
FA8650-10-D-5210-0036

**5b. GRANT NUMBER**

**5c. PROGRAM ELEMENT NUMBER**
62102F

**6. AUTHOR(S)**
1) James L. Blackshire and Shaun L. Freed – AFRL/RX
2) Jeong K. Na – Wyle

**5d. PROJECT NUMBER**
4347

**5e. TASK NUMBER** 0036

**5f. WORK UNIT NUMBER**
X0XS

**7. PERFORMING ORGANIZATION NAME(S) AND ADDRESS(ES)**
1) AFRL/RX
Wright-Patterson Air Force Base, OH 45433
2) Wyle, Aerospace Group
2700 Indian Ripple Road
Dayton, OH 45440

**8. PERFORMING ORGANIZATION REPORT NUMBER**

**9. SPONSORING/MONITORING AGENCY NAME(S) AND ADDRESS(ES)**
Air Force Research Laboratory
Materials and Manufacturing Directorate
Wright-Patterson Air Force Base, OH 45433-7750
Air Force Materiel Command
United States Air Force

**10. SPONSORING/MONITORING AGENCY ACRONYM(S)**
AFRL/RXCA

**11. SPONSORING/MONITORING AGENCY REPORT NUMBER(S)**
AFRL-RX-WP-JA-2016-0328

**12. DISTRIBUTION/AVAILABILITY STATEMENT**
Distribution Statement A. Approved for public release: distribution unlimited.

**13. SUPPLEMENTARY NOTES**
PA Case Number: 88ABW-2015-4984; Clearance Date: 15 Oct 2015. This document contains color. Journal article published in AIP Conference Proceeding, Vol. 1706, 10 Feb 2016. © 2016 AIP Publishing LLC. The U.S. Government is joint author of the work and has the right to use, modify, reproduce, release, perform, display, or disclose the work.
The final publication is available at http://dx.doi.org/10.1063/1.4940500

**14. ABSTRACT** ***(Maximum 200 words)***
Peak amplitudes of mode converted shear wave signals back scattered from macro-texture regions (MTRs) in an aerospace grade titanium alloy material are measured to be about the same level as corner trapped shear wave signals. In addition to the abnormally high shear wave responses, the time of flight data indicates that the MTR signals are back scattered from a location deep in the sample so that the round trip travel time is close to that of corner trapped signals. In this work, these two ultrasonic properties of an MTR in a test specimen cut from a titanium jet engine disk are closely studied to understand the root cause of abnormally high shear wave responses. Based on the amplitude and time of flight data collected in a laboratory condition, a decision has been made to investigate further experimentally and computationally how surface irregularity of an acoustically reflective surface affects incoming shear waves upon reflection. Attempts are made to correlate the localized back scattered signal response of the MTR in the test specimen to the beam focusing effect of a non-planar surface of an acoustically impedance mismatched boundary layer such as a fatigue crack face.

**15. SUBJECT TERMS**
Titanium; Time of flight mass spectrometry; Mechanical waves; Acoustical effects; Surface acoustic waves

| 16. SECURITY CLASSIFICATION OF: | | | 17. LIMITATION OF ABSTRACT: | 18. NUMBER OF PAGES | 19a. NAME OF RESPONSIBLE PERSON (Monitor) |
|---|---|---|---|---|---|
| a. REPORT | b. ABSTRACT | c. THIS PAGE | | | James Blackshire |
| Unclassified | Unclassified | Unclassified | SAR | 11 | 19b. TELEPHONE NUMBER *(Include Area Code)* (937) 255-0198 |

# Effect of Irregularity in Shape and Boundary of a Macro-Texture Region in Titanium

Jeong K. Na[2, a)], James L. Blackshire[1, b)], and Shaun L. Freed[1, c)]

[1]*Air Force Research Lab (AFRL/RXCA), Wright-Patterson AFB, OH 45433*
[2]*Wyle, Aerospace Group, 2700 Indian Ripple Road, Dayton, OH 45440*

[a)]Corresponding author: jeong.na@wyle.com
[b)]james.blackshire@us.af.mil
[c)]shaun.freed@wyle.com

**Abstract.** Peak amplitudes of mode converted shear wave signals back scattered from macro-texture regions (MTRs) in an aerospace grade titanium alloy material are measured to be about the same level as corner trapped shear wave signals. In addition to the abnormally high shear wave responses, the time of flight data indicates that the MTR signals are back scattered from a location deep in the sample so that the round trip travel time is close to that of corner trapped signals. In this work, these two ultrasonic properties of an MTR in a test specimen cut from a titanium jet engine disk are closely studied to understand the root cause of abnormally high shear wave responses. Based on the amplitude and time of flight data collected in a laboratory condition, a decision has been made to investigate further experimentally and computationally how surface irregularity of an acoustically reflective surface affects incoming shear waves upon reflection. Attempts are made to correlate the localized back scattered signal response of the MTR in the test specimen to the beam focusing effect of a non-planar surface of an acoustically impedance mismatched boundary layer such as a fatigue crack face. From the current experimental and computational results on the reflection of corner trapped shear waves from a concave shaped section of a non-planar crack face and the time of flight data, it is speculated that the root cause of the abnormally high peak amplitude MTR signal is possibly due to the beam focusing effect caused by the shape of the MTR.

## INTRODUCTION

The original development of key relationships defining scattering regimes in relation to the wavelength of ultrasonic waves propagating and scattering in polycrystalline materials was led by Mason [1,2], Papadakis [3-5], and Stanke-Kino [6]. These key relationships have been used as a means for estimating material properties such as statistical mean grain size under simplified materials assumptions such as single phased materials, equiaxed grains, randomly oriented crystallites, and weakly scattering heterogeneity [3-6]. For modern titanium alloys, however, the frequency-dependent, mean-field response simply breaks down because of regions of microstructure in which crystallites oriented in a common crystallographic direction over an extended length scale [7-11], often known as macro-texture regions (MTRs).

In this work, a combination of experimental measurements and forward computational models were used to study the scattering of elastic waves within a polycrystalline titanium alloy material containing MTRs. An emphasis is placed on investigating mode converted shear wave interactions with a macro-texture feature in a titanium test specimen cut from a jet engine disk material. A series of experimental measurements were made to correlate abnormally high level of amplitude signals scattered from the MTR to a geometrical focusing effect of a non-planar reflective surface. A preliminary two-dimensional forward model result showed direct insight into the possibility of focusing effect due to concave shaped surface irregularities of an acoustically impedance mismatched boundary. As a future work, the necessity of developing a three-dimensional forward model is emphasized.

*42nd Annual Review of Progress in Quantitative Nondestructive Evaluation*
AIP Conf. Proc. 1706, 050001-1–050001-9; doi: 10.1063/1.4940500

## DETECTION OF BACK SCATTERED SHEAR WAVE SIGNALS

An immersion technique was used in a laboratory condition to detect back scattered shear wave signals from an aerospace grade titanium test specimen containing an MTR. This specific test specimen, with physical dimensions of 6 mm x 8 mm x 38 mm, had previously shown a localized enhanced backscatter return signal for a mode-converted shear wave inspection process. In this work, a series of experiments and forward models were conducted to help understand and determine the root-cause of the backscatter response. To achieve this, an immersion test system was set up as shown in Figure 1(a). In this set up, the probe was set to have a 16° of launch angle and it was scanned with a high resolution 2-axis stage while the test sample was kept stationary. The probe shown in Figure 1(a) is a custom designed 10 MHz focused immersion transducer with a beam focal size between 1-2 mm in diameter at a focal point 30 mm. The peak amplitude image shown in Figure 1(b) depicts the focal zone characteristics of the immersion beam, where -6dB levels are highlighted.

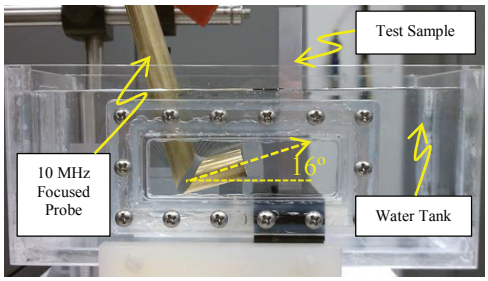


(a) Immersion set up

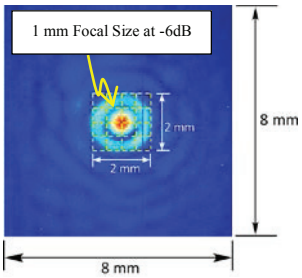


(b) Ultrasonic beam pattern at focal point

**FIGURE 1.** An immersion tank with a custom designed 10 MHz focused ultrasonic probe used for the current mode converted shear wave detection and the beam pattern of the immersion focused probe at the focal point of 30 mm.

With the immersion set up, three different locations of the titanium test sample were targeted as shown in Figure 2(a). Figure 2(b) shows the A-scan data for these three locations. It is noticeable that the edge signal appears at about 31 μsec indicating the water path length was approximately 23 mm. Both the MTR and corner trapped signals appear between 36 and 38 μsec and the time difference between these two signals is estimated to be about 1.7 μsec. From this travel time information, it can be assumed that the MTR signal is back scattered from a location slightly less deep than the location from where the corner trapped signal reflects back. It should be noted that the amplitude of MTR signal is higher than the corner trapped signal, where the oval shaped c-scanned image of the hot-spot section shown in Figure 2(c) suggests that the reflective MTR surface is a non-planer, concave shape causing signal enhancement through local beam focusing effects [11].

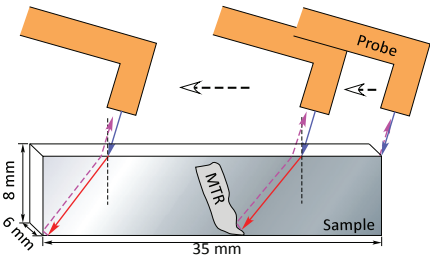


(a) Three different locations

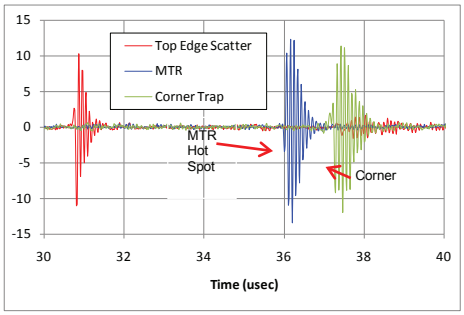


(b) A-scan data for three different locations

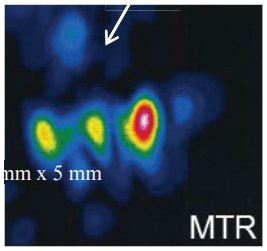


(c) C-scan image of MTR

**FIGURE 2.** Mode converted shear wave test results for three different locations of the rectangular shaped titanium test specimen; top edge, MTR and corner trapped signals.

## EFFECT OF SURFACE IRREGULARITY: EXPERIMENT

Based on the results of the immersion testing described in the previous section, a series of experiments were accomplished to investigate shear wave interactions with planar and non-planar corner-traps. The diagram in Figure 3(a) depicts a typical corner-trap condition with two perpendicular surfaces. In this case, a focused oblique incident longitudinal wave (L-wave) in water converts into a shear wave (S-wave) and transmits into the solid test material with a refractive angle of $\theta_R$. After reflection from the bottom surface of material, the wave interacts with the vertical surface so that the wave reflects back to the top surface at an incident angle of $\theta_R$. Mode conversion occurs at the top surface creating an L-wave that propagates back in water to the transducer. It should be noted that the lower portion of the vertical surface of the test material, as indicated in Figure 3(a), is the surface area of interest for the current investigation to understand how a shear wave interacts with a non-planar surface. Before testing was conducted on a complex surface morphology, an isotropic amorphous plate glass was first tested as a reference material for the corner trapped shear wave detection experiment. Figure 3(b) depicts photos of the 6 mm thick reference glass sample having an aerial dimension of 30 mm x 70 mm. One of the narrow sides of the glass plate was lapped and polished to be flat to a 3 μm finish with sharp, 90° corner edges.

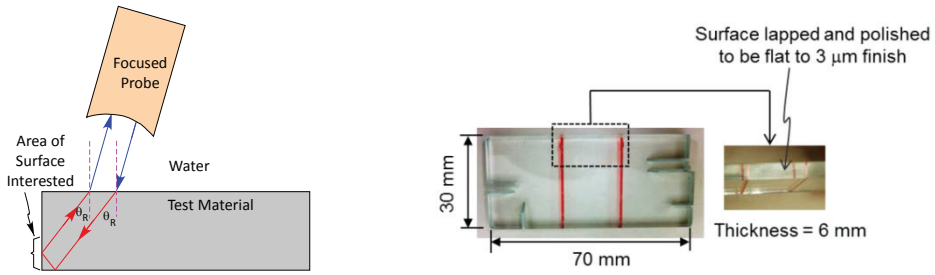


(a) Corner trapped signal detection (b) Reference glass plate

**FIGURE 3.** A corner trapped signal detection condition for a shear wave in an immersion NDE method and photos of a glass plate used as a reference test sample for the immersion corner trap experiment.

The same custom designed 10 MHz immersion probe was used for the corner trapped signal testing using the glass plate reference sample. The beam was focused on the back corner surface using a 16° incidence angle in water relative to the surface normal generating a mode-converted shear wave in the material. A 2-dimensional raster scan of the transducer in the corner-trap region was then accomplished as illustrated in Figure 4(a). Figure 4(b) shows the C-scan image result of the peak amplitude distribution for the corner trapped signals scanned over an area of 8 mm x 16 mm. The bright horizontal band in the middle of the image is the corner-trap signal response, having a width of 1.2 mm. This measured value is close to the size of ultrasonic beam diameter at the focal point as shown in Figure 1(a). In addition, there are no noticeable scattering, distortion, focusing or defocusing effects. This image result demonstrates how a corner-trapped signal behaves when a small diameter shear wave beam is focused on a sharp 90° corner for an isotropic amorphous material having smooth planar reflective surfaces.

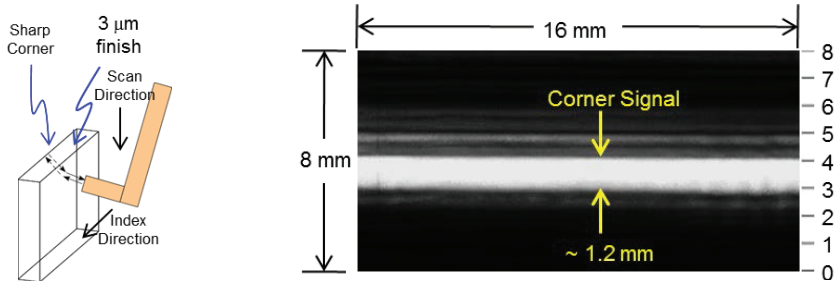


(a) Scan scheme (b) Peak amplitude C-scan image of corner trapped signal for glass plate

**FIGURE 4.** Corner-trapped shear wave signal detection on a 6 mm thick reference glass plate and its amplitude C-scan image.

A similar experiment was conducted with an aluminum block containing a vertically grown surface breaking crack induced by a three point bending fatigue test method. The physical dimensions of the test sample were 12 mm thick, 20 mm wide and 95 mm long and the location of the fatigue crack was in the midsection of the sample. To minimize any sample geometrical and surface roughness effects for the mode converted shear wave testing, both the top and bottom surfaces (20 mm x 96 mm) were lapped to be flat to a 3 mm finish and the final parallelism of the two finished surfaces was measured to be less than 5 μm across the whole length of 96 mm.

Before the two crack faces were scanned for their corner trapped signals, one of the side surfaces was lapped and polished to be flat to a 3 μm finish and scanned as illustrated in Figure 5(a). The C-scan image of the test result is shown in Figure 5(b). One can notice that this corner trapped signal image is different from the C-scan image of the reference glass plate sample depicted in Figure 4(b). A local, higher-amplitude region can be seen in the Figure 5(b) image (between the two dotted horizontal lines), which represents the primary corner-trapped signal region. Relative to the glass plate case, the spatial pattern is irregular showing discrete intensified return signal regions. Additionally, the upper area above the corner-trapped signal location shows an extended region of signal amplitudes. Considering both the horizontal and vertical reflective surfaces are flat and have 3 μm finishes, this amplitude pattern is thought to be due to microstructure heterogeneity in the aluminum material.

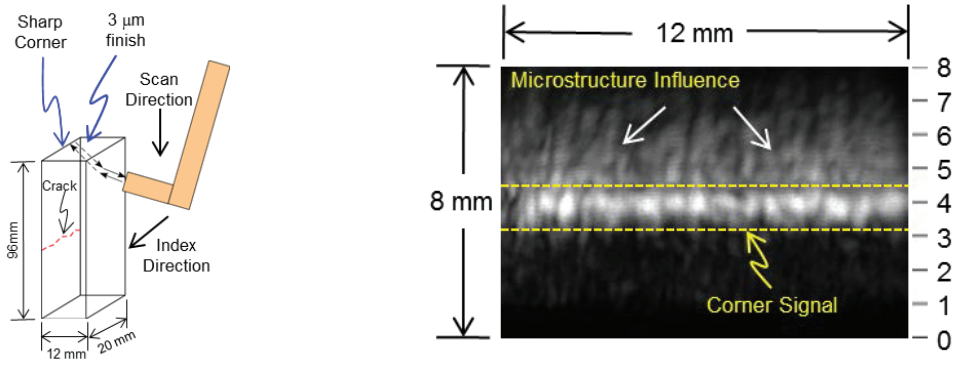


(a) Scan scheme (b) Peak amplitude C-scan image of corner trapped signal for aluminum

**FIGURE 5.** Corner trapped shear wave signal detection on a 12 mm thick aluminum sample and its amplitude C-scan image.

After the corner-trapped signal testing for planar 90° surface conditions was completed, an investigation of irregular crack morphology was accomplished in the middle of the sample to understand how non-planer surfaces reflect incoming shear waves. The optical image in Figure 6 shows the crack root on the bottom surface of the aluminum block, with the schematic diagram showing the sample dimensions and location of the crack feature. The relatively straight section of the crack in the middle, indicated by the dotted-lined box, was scanned for the corner trapped signal detection experiment.

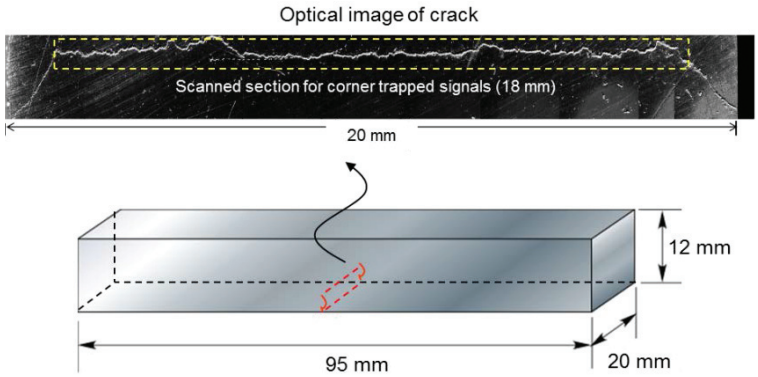


**FIGURE 6.** An optical image of the 3-point bending fatigue crack taken from the bottom surface of the aluminum sample and a schematic diagram of the sample to show how the crack is assumed to be vertically oriented.

The two schematic diagrams and C-scan image results shown in Figure 7 illustrate how the irregular fatigue crack faces were scanned for their corner trapped signals. During the course of experiment, only the sample was flipped

vertically and all the scan parameters such as probe standoff distance, scan direction, and beam incidence angle were kept the same for both crack faces. The scan size was set to be 18 mm x 18 mm to cover the midsection of the crack as described above, where the internal crack face surfaces were assumed to be normal to the bottom reflecting surface creating a 90° corner-trap condition.

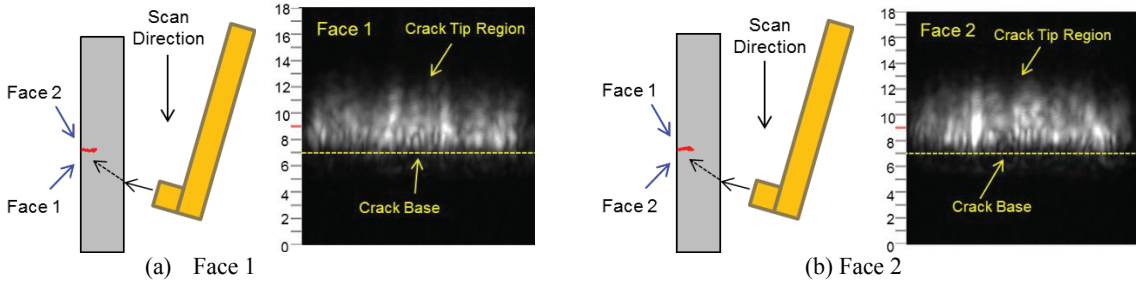


**FIGURE 7.** Peak amplitude C-scan images of corner trapped signals for the two fatigue crack faces.

Figure 8 provides a direct comparison of the two C-scan images from Figure 7, and the optical image of the crack root from Figure 6, where the same length scales are used. A comparison of the three images in Figure 8 shows a concave crack morphology feature towards the left half of the optical image, which correlates reasonably well with an intensified elongated C-scan response for crack Face 2, and a reduced signal response for the same region in the Face 1 image. Although qualitative in nature, the results suggest local beam focusing and de-focusing may be occurring due to local irregular surface conditions in a corner-trap response.

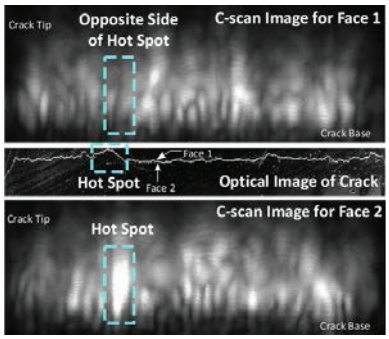


**FIGURE 8.** Comparison of the peak amplitude C-scan images of Face 1 and Face 2 corner trapped signals reflected from non-planar fatigue crack surfaces of the fatigued aluminum sample.

## EFFECT OF SURFACE IRREGULARITY: COMPUTATIONAL MODELING

To better understand the impact of local surface morphology on reflected ultrasonic fields, a two-dimensional forward model was developed using the commercially available PZFlex software package. The purpose was to understand how idealized ultrasonic plane waves interact with planar and non-planer surfaces in a two-dimensional configuration. For the non-planar case, the optical image crack morphology in Figure 6 was used to generate a reflective surface in the forward model as depicted in Figure 9(b).

The models included an ideal lossless medium (aluminum) with the reflecting surfaces being air. A 1-cycle, sinusoidal pressure loading condition was applied normal to the right surface of the model, with outer surfaces having free boundary conditions as indicated in Figure 9. The ultrasound wavelength was chosen to be the approximate size of the local morphology features (1 mm).

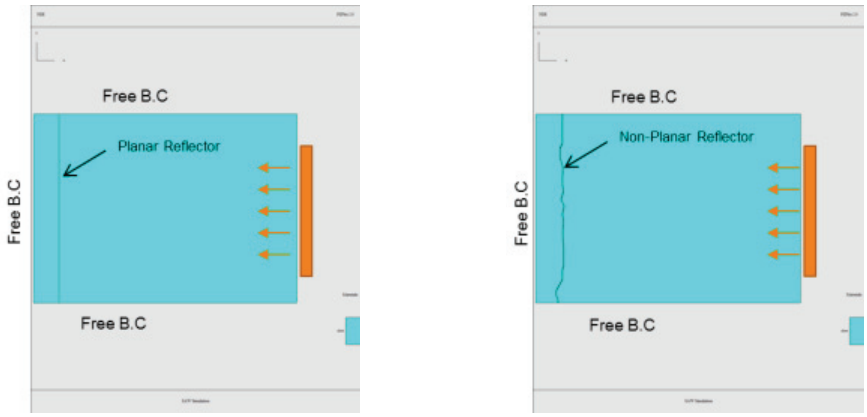


(a) Planar case (b) Non-planer case

**FIGURE 9.** Two dimensional models used to investigate ultrasonic beam reflection from a planar and non-planar surface.

Computational model results of both planar and non-planar cases are shown in Figure 10. From these results, one can notice that the incident wave gets 180º phase shift upon reflection as indicated in the time domain amplitude variation graphs. These time domain graphs represent the dotted line drawn along the centerline of each corresponding 2-D amplitude distribution image shown above each graph. For the non-planar case, Figure 10(b), the reflected wave has a slightly lower peak-to-peak amplitude value than the planar case and it is due to scattering of energy from the non-planar reflective surface condition. This wave scattering phenomenon is more pronounced when the two peak amplitude field images shown on the right hand side are compared. For the non-planar case, there are several local regions showing beam focusing effects from the concave sections of the reflective surface. The zoomed-in image in Figure 10(b) shows at least four concave sections inducing beam focusing effects.

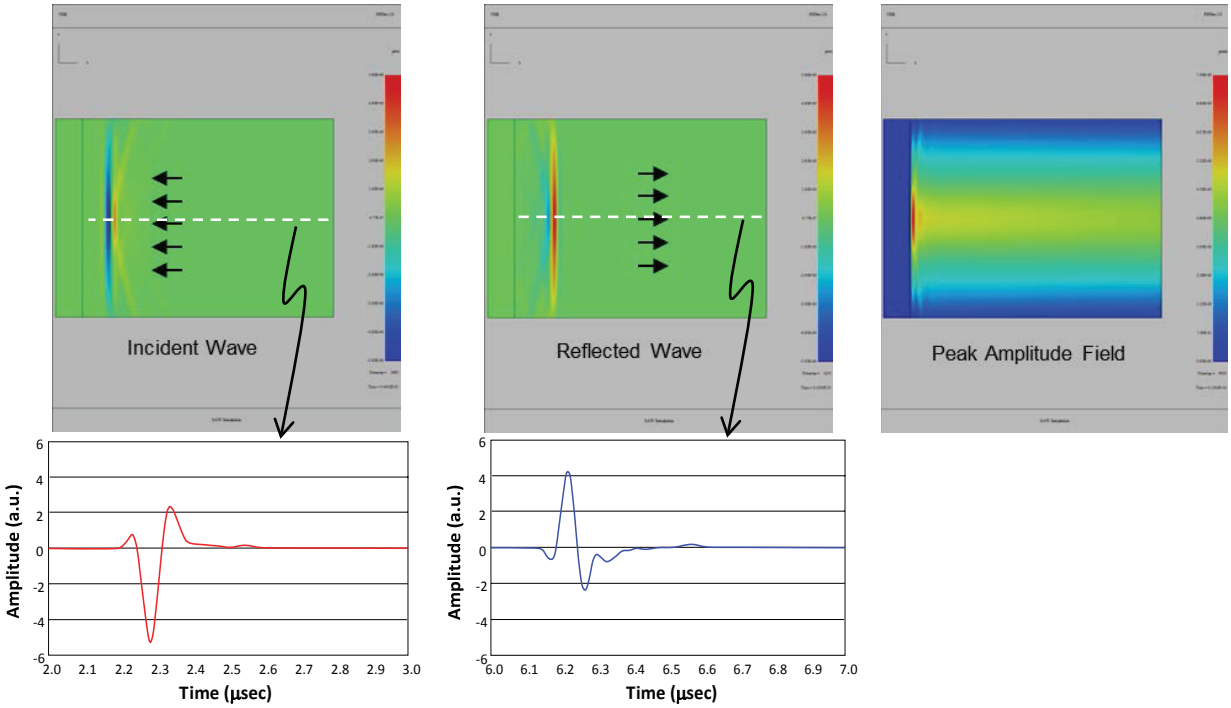


(a) Planar Reflector Case

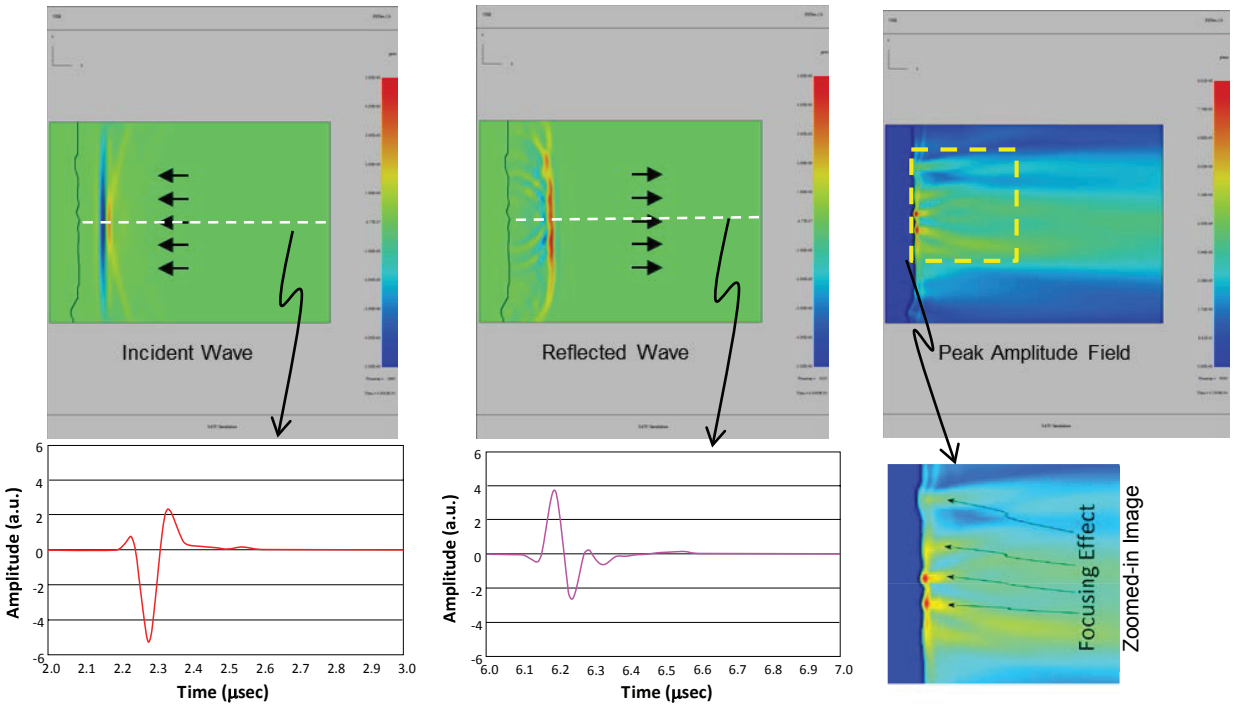


(b) Non-planar Reflector Case

**FIGURE 10.** Computational modeling results for planar and non-planar reflective surface conditions.

## DISCUSSION

Figure 11 shows a schematic diagram of the original titanium test sample that motivated the current research. The figure depicts the titanium sample, its dimensions, and corresponding electron backscatter diffraction (EBSD) image overlaid on its side. The microstructure feature near the middle of the side-profile image is thought to be responsible for the high peak amplitude shear wave response in the C-scan image shown below the EBSD image. The local morphology of the microstructure feature suggests a local corner-trap condition may be present. Shear wave round trip times for the corner-trap on the left, and the microstructure feature in the center of the sample were estimated to be 6.38 µsec and 4.58 µsec, respectively, where the time difference of 1.8 µsec between these two signals is close to the time difference of 1.7 µsec that was provided in the A-scan results in Figure 2(b). The signal strengths of the corner-trap and microstructure response were similar, however, which requires a strong impedance boundary mismatch in both cases. The local morphology reflection studies conducted in this paper provide one possible explanation for the strong microstructure response relative to the corner trap response, where beam focusing and de-focusing may be occurring. Additional models and experiments are being conducted to answer these questions.

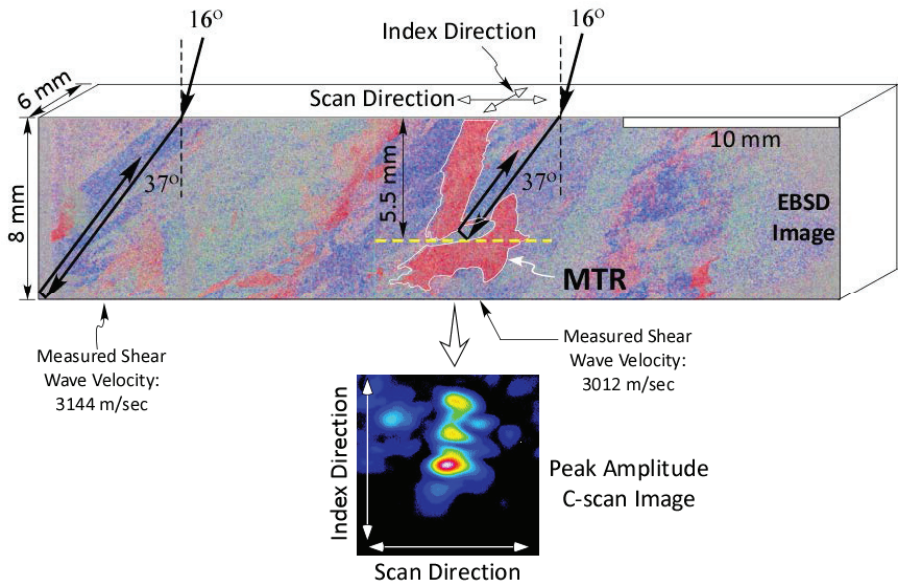


**FIGURE 11.** A schematic drawing showing an EBSD image taken from the side of titanium test sample and its corresponding ultrasonic peak amplitude C-scan image of back scattered shear waves.

## CONCLUSION AND FUTURE WORK

A titanium test specimen with complex morphology microstructure features showed strong backscatter signal levels which were similar to corner trapped signals. Based on EBSD image analysis and time-of-flight measurements, the location of a reflective microstructure surface was estimated to be slightly above the bottom surface of the test sample. The peak amplitude C-scan image suggests that the reflective surface within the material may have a three dimensional non-planar concave-shaped, impedance-mismatched boundaries, generating potential beam focusing effects.

The influence of surface morphology on beam focusing effects was investigated experimentally by an immersion corner trapped shear wave detection method on a vertically grown fatigue crack having a complex surface irregularity. The results showed that a local concave-convex section of a crack face did indeed induce a localized beam focusing effect upon reflection. The beam focusing effect was simulated computationally with an idealized 2-dimensional forward model using a plane wave interacting with a complex surface irregularity. The experimental and forward model results support the hypothesis that local microstructure morphology may produce enhanced signal levels due to beam focusing effects.

Future planned work includes a layer by layer sectioning of the titanium sample, and 3-dimensional EBSD microstructure characterization to understand microstructure morphology effects on ultrasound response for improved NDE microstructure characterization.

## ACKNOWLEDGMENT

This research was funded by AFRL's Venture Project FA8650-10-D-5210, Task Order TO36 through the Universal Technology Corporation in Dayton, Ohio.

## REFERENCES

1. W.P. Mason and H.J. McSkimin, J. Acoust. Soc. Am., **19 (3)**, 464-473, (1947).
2. W.P. Mason and H.J. McSkimin, J. Appl. Phys., **19**, 940-946, (1948).

3. E. Papadakis, J. Appl. Phys., **35 (5)**, 1586-1594, (1964).
4. E. Papadakis, J. Acoust. Soc. Am., **37 (4)**, 703-710, (1965).
5. E. Papadakis, J. Appl. Phys., **36 (5)**, 1738-1740, (1965).
6. F.E. Stanke and G.S. Kino, J. Acoust. Soc. Am., **75**, 665–681, (1984).
7. A. Moreau, L. Toubal, P. Bocher, M. Humbert, E. Uta, and N. Gey, Mat. Char. **75**, 115-128, (2013).
8. A. Bhattacharjee, A.L. Pilchak, O.I. Lobkis, J.W. Foltz, S.I. Rokhlin, and J.C. Williams, Met. and Mat. Trans. A., **42A**, 2358-2372, (2011).
9. A.L. Pilchak, J. Li, and S.I. Rokhlin, Met. and Mat. Trans. A., **45 (10),** 4679-4697, (2015).
10. F.J. Margetan, M. Gigliotti, L. Brashe, and W. Leach, U.S. DOT/FAA Report AR-02/114, 34-35, (2002).
11. J.L. Blackshire, 2012 IEEE International Ultrasonics Symposium, 248-251, (2012, October).